

Impact of Concentration measurements upon estimation of flow and transport parameters: the lagrangian approach.

Original

Impact of Concentration measurements upon estimation of flow and transport parameters: the lagrangian approach / Dagan, G.; Butera, Ilaria; Grella, E.. - In: WATER RESOURCES RESEARCH. - ISSN 0043-1397. - STAMPA. - 32:(1996), pp. 297-306. [10.1029/95WR02716]

Availability:

This version is available at: 11583/1397754 since:

Publisher:

AGU

Published

DOI:10.1029/95WR02716

Terms of use:

This article is made available under terms and conditions as specified in the corresponding bibliographic description in the repository

Publisher copyright

(Article begins on next page)

Impact of concentration measurements upon estimation of flow and transport parameters: The Lagrangian approach

Gedeon Dagan

Faculty of Engineering, Tel Aviv University, Tel Aviv, Israel

Ilaria Butera and Elisabetta Grella

Department of Hydraulic Engineering, Milan Polytechnic, Milan, Italy

Abstract. Transport of a conservative solute takes place in a heterogeneous formation of spatially variable conductivity. The latter is modeled as a random space function of stationary lognormal distribution. As a result the velocity field and the concentration are also random. Assuming that measurements of concentration of an existing plume are available, the problem addressed here is to assess their effect upon identification of log conductivity and flow transport variables. The solution is sought in a Lagrangian framework in which transport is represented in terms of the random trajectories of particles originating from the initial plume. A concentration measurement is equivalent to the passage of a trajectory through the measurement point at a given time. The impact of measurements is achieved by conditioning any variable of interest on realizations for which at least one trajectory satisfies the requirement. It is shown that cokriging of concentration and another flow or transport variable leads to the correct conditioned mean of the latter. In contrast, the conditional variance based on cokriging is erroneous. The procedure is illustrated for two-dimensional flow under a few simplifying assumptions. The effect of a concentration measurement upon the expected value and variance of log transmissivity and plume centroid are examined in a few particular cases. The procedure may improve the solution of the inverse problem and the prediction of transport of existing plumes.

1. Introduction

Natural porous formations are as a rule heterogeneous, their hydraulic conductivity or transmissivity varying in space over orders of magnitude. Field studies and theoretical investigations have led to the conclusion that these and the associated velocity variations constitute the main mechanism of solute spreading in subsurface transport. Because of the irregular spatial distribution and the uncertainty affecting it, it is common to model the conductivity as a random space function and similarly for the dependent variables such as water head, velocity, and solute concentration.

One of the major aims of transport models is to derive the statistical moments of the concentration (mean, variance, and spatial and temporal correlation) as functions of the given statistics of the conductivity and of given flow and transport initial and boundary conditions. Various approximate models, of an analytical or a numerical nature, have been developed in the past in order to achieve this goal.

Transport models can be classified as based on unconditional or conditional probabilities. In the first case, measurements of conductivity and heads are used in order to identify the statistical moments and their stationary probability distribution functions, and this is the input information for the transport model. In the second case the conductivity and head statistical moments are conditioned on the actual measurements, for example, by cokriging. As a result they are no longer

stationary random variables, and the same is true for the concentration. Conditioning is expected to improve prediction by reducing its uncertainty, and it is most effective for transmissivity large-scale variations.

Another classification relevant to the present study is related to the representation of transport within Eulerian and Lagrangian frameworks. In the first approach the concentration is determined by solving the partial differential equation of convection-dispersion, with the flow velocity being a random space function related to the conductivity. In the Lagrangian methodology, known as particle tracking in its numerical version, the solute body is regarded as a collection of particles, and the process is represented in terms of their random trajectories. Most of the literature on subsurface transport deals with prediction of concentration distribution or of plume spatial moments for given conductivity probability distribution, either unconditional or conditional.

In many applications, field measurements include those of concentrations of existing plumes. The question is whether these additional data can be employed for better identifying the conductivity statistics, in an inverse procedure, or for predicting the subsequent evolution of the plume. The aim of the present study is to investigate this topic within the Lagrangian framework and by using conditional probability.

To our knowledge the subject has received less attention than the prediction based only on conductivity or head data. The problem was addressed in an Eulerian framework by *Graham and McLaughlin* [1989a, b]. They truncate the transport equations at first order in the conductivity variance and derive subsequently partial differential equations for the two-point

concentration-velocity cross covariance and for the concentration covariance. These equations are integrated numerically in the unconditional case [Graham and McLaughlin, 1989a] and in association with an extended Kalman filter in the conditional mode [Graham and McLaughlin, 1989b]. In the latter case a few final results are presented for a two-dimensional particular case.

Although the pioneering work of Graham and McLaughlin [1989a, b] sets concentration conditioning in a comprehensive and rational framework, there are a few open issues which are addressed in a different manner in the present study. First, the Eulerian truncation has been found to be questionable, at least in a few circumstances [Dagan and Neuman, 1991]. Second, the procedure is similar to cokriging, and it is mostly appropriate for normal variables, which is not the case with concentration (see section 3). Last, unlike Graham and McLaughlin [1989a, b], we shall try to analyze here in a simple and systematic manner the impact of concentration measurements, rather than in a particular case of a complex configuration.

The impact of concentration measurements has been addressed under similar basic assumptions by Deng *et al.* [1993a, b] and by Lee *et al.* [1993]. These authors employ concentration measurements in order to identify the underlying statistical structure of the conductivity through solute plume spatial moments. Though the methodology is somewhat different from that of Graham and McLaughlin [1989a, b], the same general comments apply to these studies as well. Within the Lagrangian approach, conditioning of plume centroid and second spatial moments has been investigated for conductivity and head measurements [Dagan, 1984; Rubin, 1991], and similarly for travel time to a control plane [Rubin and Dagan, 1992].

The present study is an extension of this approach to concentration data. Our main aim here is to develop the methodology and to illustrate it in a simple manner, in order to grasp the impact of concentration measurements. Further applications to more complex cases are outlined in section 6.

2. Mathematical Statement of the Problem and Its Qualitative Analysis

We consider a formation of conductivity or transmissivity $K(\mathbf{x})$ of stationary lognormal distribution. With $Y = \ln K$ the entire spatial structure of Y is embedded in $\langle Y \rangle = m_Y$ and $C_Y(\mathbf{r}) = \langle Y'(\mathbf{x})Y'(\mathbf{y}) \rangle = \sigma_Y^2 \rho_Y(\mathbf{r})$, $\mathbf{r} = \mathbf{x} - \mathbf{y}$. Here \mathbf{x} and \mathbf{y} are Cartesian coordinate vectors, angle brackets stand for ensemble mean, σ_Y^2 is the variance, and ρ_Y is the autocorrelation. The flow is uniform in the mean, with velocity $\mathbf{V}(\mathbf{x}) = \mathbf{U} + \mathbf{u}(\mathbf{x})$, where $\mathbf{U} = \langle \mathbf{V} \rangle = \text{const}$ and the random fluctuation \mathbf{u} is characterized in its various moments, e.g., $u_{ij}(\mathbf{r}) = \langle u_i(\mathbf{x})u_j(\mathbf{y}) \rangle$. At $t = 0$ a solute body of concentration $C_0 = \text{const}$ is injected in a volume (area) A_0 . The transport problem is to derive the random function $C(\mathbf{x}, t)$, the concentration distribution in space and time.

In the Lagrangian, or in the particle tracking approach, the plume is regarded as a collection of particles moving along random trajectories $\mathbf{x} = \mathbf{X}_i(t; \mathbf{a})$. The basic equations are [e.g., Dagan, 1989, section 4.3]

$$\frac{d\mathbf{X}_i}{dt} = \mathbf{U} + \mathbf{u}(\mathbf{X}_i) + \mathbf{u}_d \quad \mathbf{X}_i(0, \mathbf{a}) = \mathbf{a} \quad (1)$$

$$C(\mathbf{x}, t) = C_0 \int_{A_0} \delta[\mathbf{x} - \mathbf{X}_i(t; \mathbf{a})] d\mathbf{a} \quad (2)$$

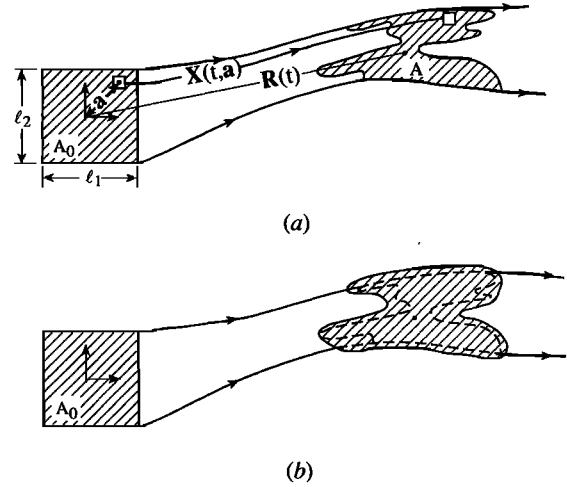


Figure 1. Schematic representation of the solute body motion: (a) advective transport and (b) plume extent as affected by pore-scale dispersion.

In the first equation, $\mathbf{u}(\mathbf{x})$ is the fluctuation of the given random velocity field, while \mathbf{u}_d stands for the velocity of a “Brownian motion,” i.e., a Wiener process, associated with pore-scale diffusion. In equation (2) the Dirac operator δ stipulates that at time t a particle of mass $C_0 d\mathbf{a}$ originating at $t = 0$ is at $\mathbf{x} = \mathbf{X}_i$ (Figure 1). Since $\mathbf{u}(\mathbf{x})$ and \mathbf{u}_d are random, the solution \mathbf{X}_i is also random, of the probability density function (pdf) $f(\mathbf{X}_i; t, \mathbf{a})$. Knowledge of f leads immediately to

$$\langle C(\mathbf{x}, t) \rangle = \int C(\mathbf{x}, t) f(\mathbf{X}_i) d\mathbf{X}_i = C_0 \int_{A_0} f(\mathbf{x}; t, \mathbf{a}) d\mathbf{a} \quad (3)$$

while the variance σ_c^2 requires determining $f(\mathbf{X}_i, \mathbf{Y}_j; t, \mathbf{a}, \mathbf{b})$, the joint pdf of trajectories at time t of two particles originating at $\mathbf{x} = \mathbf{a}$ and $\mathbf{x} = \mathbf{b}$ within A_0 at $t = 0$, respectively.

The basic equations (1) and (2) may be also employed in order to derive the statistical moments of other entities, such as the plume spatial moments

$$\mathbf{R}(t) = \frac{1}{A_0} \int_{A_0} \mathbf{x} C(\mathbf{x}, t) d\mathbf{x} \quad (4)$$

$$S_{ij}(t) = \frac{1}{A_0} \int_{A_0} (x_i - R_i)(x_j - R_j) C(\mathbf{x}, t) d\mathbf{x}$$

where \mathbf{R} is the centroid coordinate and S_{ij} ($ij = 1, 2, 3$) are second spatial moments. By the same token one may consider $C_{YC} = \langle Y'(\mathbf{x})C(\mathbf{y}, t) \rangle$, the log conductivity-concentration cross covariance, $C_{u,C} = \langle u_i(\mathbf{x})C(\mathbf{y}, t) \rangle$, the velocity-concentration cross covariance, and so on. If the starting point in (1) is the stationary velocity $\mathbf{u}(\mathbf{x})$, the resulting moments $\langle C \rangle$, σ_C^2 , $\langle \mathbf{R} \rangle$, R_{ij} , $\langle S_{ij} \rangle$, C_{YC} , \dots are the unconditional ones.

We assume now that measurements of C at a few points $\mathbf{x} = \alpha_n$ and times $t = \tau_n$ ($n = 1, 2, \dots, N$) are available, i.e., $C(\alpha_n, \tau_n)$ are given. Then the mathematical problem pursued here can be stated in a general manner as follows: Determine the statistical moments $\langle Y^c(\mathbf{x}|\alpha_n, \tau_n) \rangle$, $\sigma_Y^{2,c}(\mathbf{x}|\alpha_n, \tau_n)$, $\langle \mathbf{R}^c(t|\alpha_n, \tau_n) \rangle$, \dots , for C satisfying equations (1) and (2), conditioned on the values $C(\alpha_n, \tau_n)$. In other words, the conditional moments are determined by using the subensemble

of realizations of the velocity fields for which C has the prescribed values at α_n, τ_n .

An exact solution of both the unconditional and conditional problems is not feasible, and we adopt here a few simplifying assumptions. First, we neglect in (1) the effect of pore-scale dispersion, rewriting (1) as

$$\frac{d\mathbf{X}}{dt} = \mathbf{U} + \mathbf{u}(\mathbf{X}) \quad (5)$$

The effect of this far-reaching assumption, together with that of steady flow of divergence free velocity, is that the concentration stays constant and equal to C_0 and the volume (area) A of the solute body is also preserved (Figure 1a). Thus the randomness of the velocity field manifests itself in the trajectory of the plume centroid and in the change of its shape. In the past the justification of this assumption was that the second spatial moments S_{ij} (4) of the solute body are determined mainly by the randomness of \mathbf{u} and to a much lesser extent by pore-scale dispersion. This assumption has been found to be quite accurate for high Pe numbers, depending on the anisotropy ratio of heterogeneity [Neuman *et al.*, 1987]. However, pore-scale dispersion may have an important effect upon σ_C^2 , owing to the local dilution effect. Thus, while field measurements display the irregular spatial variations of C caused by heterogeneity, concentrations do not maintain their initial value.

The salient question is whether pore-scale dispersion has a significant effect upon the conditioning of the log transmissivity Y or the plume centroid \mathbf{R} by measurements of C , which is the objective of the present study. While a quantitative check of this effect is yet to be carried out, we shall try to demonstrate in a qualitative manner that it is probably small. As shown in the next section, we do not condition a generic variable B , like Y or \mathbf{R} , by the concentration value itself. Instead, in the Lagrangian framework, measuring $C = C_0$ at a point is tantamount to the statement that a trajectory of a fluid particle originating from the initial solute body has reached that point (Figure 1). In practice, because of pore-scale dispersion, measured concentrations are smaller than C_0 , and the volume of the plume, defined as the volume in which $C > 0$, is larger than the initial one, which in turn is invariant under the purely advective transport [Thierrin and Kitanidis, 1994]. This dilution is achieved, however, mainly by solute being diffused into the gaps left by the purely advective transport of the various parts of the plume and in boundary layers adjacent to them (see Figure 1b). Indeed, this picture is supported by the finding that the centroid of the plume and its second spatial moments are little affected by pore-scale dispersion. It is plausible therefore that the error incurred by assuming that a fluid particle trajectory reaches a point where a measurement of C is different from zero is relatively small.

Then, for conditioning purposes the concentration field (2) can be rewritten symbolically as follows:

$$C(\mathbf{x}, t) = C_0 H(A|\mathbf{a} \in A_0) \quad (6)$$

where H is an indicator function, equal to unity within the volume (area) A determined by the manifold of trajectories $\mathbf{x} = \mathbf{X}(t, \mathbf{a})$ originating from $\mathbf{a} \in A_0$ at $t = 0$ and equal to zero otherwise (Figure 1a).

Our next simplification is to consider here conditioning by a single measurement $C = C_0$ at $\mathbf{x} = \alpha, t = \tau$. Our main task here is to establish the methodology and to examine the impact

of conditioning in a systematic manner, and these goals can be achieved more easily for one measurement (the extension to a few α_n, τ_n is discussed in section 6).

Let $B(\mathbf{x}, t)$ be a generic notation for a random variable correlated to concentration, for example, $Y(\mathbf{x}), u_i(\mathbf{x}), R_i(t), S_{ij}(t), \dots (i, j = 1, 2, 3)$. Then the mathematical problem can be stated as follows: Derive the moments of B conditioned on a measurement $C(\alpha, \tau) = C_0$, with C given by (2) or (6) and for \mathbf{X} solution of (5).

We start developing the procedure in a general manner in the following section. Additional simplifying assumptions are adopted in section 4 in order to effectively evaluate the conditional statistical moments.

3. Conditioning on Trajectories

In line with the discussion above, the presence of a measurement $C(\alpha, \tau) = C_0$ is equivalent to the statement that at least one trajectory originating from $\mathbf{a} \in A_0$ passes through $\mathbf{x} = \alpha$ at $t = \tau$. In order to give this statement a mathematical content we consider the pdf $f(\mathbf{a}; \mathbf{x}, t)$ defined as the probability density of trajectory origins \mathbf{a} at $t = 0$ that reach a given \mathbf{x} at time t . Because of the continuity equation, whose Lagrangian form is $d\mathbf{a} = d\mathbf{X}$, we have

$$f(\mathbf{a}; \mathbf{X}, t) = f(\mathbf{X}; \mathbf{a}, t) \quad (7)$$

Obviously, $\int f(\mathbf{a}; \mathbf{X}, t) d\mathbf{a} = 1$ for the entire space, since it represents the probability of reaching \mathbf{X} from anywhere.

The conditioning of trajectories stems from the finiteness of the initial solute body, i.e., from $\mathbf{a} \in A_0$. In other words the subensemble of a value underlying the conditional probability is the one for which $\mathbf{a} \in A_0$.

The conditional pdf of a random variable $B(\mathbf{x}, t)$ correlated with $X(\tau, \mathbf{a})$ is given therefore by the Bayes theorem as follows:

$$f^c(B, \mathbf{a}) = \frac{f(B, \mathbf{a}; \mathbf{x}, t, \alpha, \tau)}{\iint_{A_0} f(B, \mathbf{a}; \mathbf{x}, t, \alpha, \tau) d\mathbf{a} dB} \quad \mathbf{a} \in A_0$$

$$f^c(B, \mathbf{a}) = 0 \quad \mathbf{a} \notin A_0 \quad (8)$$

where by (7), $f(B, \mathbf{a}; \mathbf{x}, t, \alpha, \tau) = f(B, \mathbf{X} = \alpha; \mathbf{x}, t, \mathbf{a}, \tau)$. As a result we get for the conditional moments

$$\langle B^c(\mathbf{x}, t|\alpha, \tau) \rangle = \int B f^c(B) dB$$

$$\sigma_B^{2,c} = \int (B - \langle B^c \rangle)^2 f^c(B) dB \quad (9)$$

$$f^c(B) = \frac{\int_{A_0} f(B, \mathbf{a}; \mathbf{x}, t, \alpha, \tau) d\mathbf{a}}{\iint_{A_0} f(B, \mathbf{a}; \mathbf{x}, t, \alpha, \tau) d\mathbf{a} dB}$$

The results (8) and (9) can be easily connected to those of cokriging by observing that the integral of the denominator in (8) is the marginal that is equal to $\langle C \rangle / C_0$ (3). Similarly, by (2)

and (7) we have $\int_{A_0} B^m f(B, \mathbf{a}; \mathbf{x}, t, \alpha, \tau) d\mathbf{B} d\mathbf{a} = (1/C_0) \langle B^m(\mathbf{x}, t) C(\alpha, \tau) \rangle$ for any given m .

Hence we may rewrite

$$\langle B^c(\mathbf{x}, t | \alpha, \tau) \rangle = \langle B(\mathbf{x}, t) C(\alpha, \tau) \rangle / \langle C \rangle = \langle B \rangle + C_{BC} / \langle C \rangle \quad (10)$$

$$\begin{aligned} \sigma_B^{2,c}(\mathbf{x}, t | \alpha, \tau) &= \langle B^2(\mathbf{x}, t) C(\alpha, \tau) \rangle / \langle C \rangle - \langle B^c(\mathbf{x}, t | \alpha, \tau) \rangle^2 \\ &= \langle [B'(\mathbf{x}, \tau)]^2 C(\alpha, \tau) \rangle / \langle C(\alpha, \tau) \rangle \\ &\quad - [C_{BC}(\mathbf{x}, t | \alpha, \tau) / \langle C(\alpha, \tau) \rangle]^2 \end{aligned} \quad (11)$$

It can be shown that (10) is indeed identical to the outcome of cokriging B and C (2), whereas the variance (11) has an expression different from that resulting from cokriging. The reason is that C in (2) and (6) is an indicator function, whereas cokriging estimation variance is equal to the exact variance for normal variables.

Along the same lines we can derive the moments of B conditioned on a measurement $C(\alpha, \tau) = 0$. The conditional probability in (8) is replaced by

$$\begin{aligned} f^c(B, \mathbf{a}) &= \frac{\int_{A_0} f(B, \mathbf{a}; \mathbf{x}, t, \alpha, \tau) d\mathbf{a}}{1 - \int_{A_0} \int_{A_0} f(B, \mathbf{a}; \mathbf{x}, t, \alpha, \tau) d\mathbf{a} d\mathbf{B}} \\ &= \frac{\int_{A_0} f(B, \mathbf{a}; \mathbf{x}, t, \alpha, \tau) d\mathbf{a}}{1 - \langle C(\alpha, \tau) \rangle / C_0} \quad \mathbf{a} \notin A_0 \quad (12) \\ f^c(B, \mathbf{a}) &= 0 \quad \mathbf{a} \in A_0 \end{aligned}$$

This leads to the final results:

$$\langle B^c(\mathbf{x}, t | \alpha, \tau) \rangle = \langle B \rangle - C_{BC} / (C_0 - \langle C \rangle) \quad C(\alpha, \tau) = 0. \quad (13)$$

Equation (13) is identical to the one obtained by cokriging, whereas the conditional variance is given by

$$\sigma_B^{2,c} = \frac{\langle B^2 \rangle}{1 - \langle C \rangle / C_0} - \frac{\langle B^2 C \rangle}{C_0 - \langle C \rangle} - (\langle B^c \rangle)^2 \quad C(\alpha, \tau) = 0 \quad (14)$$

The conditional variance (14) is generally different from (11), contrary to the results based on cokriging.

Equation (9) or equations (10) and (11) will serve in the following sections in order to examine the impact of $C(\alpha, \tau) = C_0$ upon various random variables B . In view of the previous discussion we observe that for $A_0 \rightarrow \infty$, $\int_{A_0} f(B, \mathbf{a}) d\mathbf{a} d\mathbf{B} = 1$, and the conditional pdf in (8) tends to the unconditional one. In contrast, for $A_0 \rightarrow 0$, $f^c(B, \mathbf{a})$ tends to a Dirac function.

4. Conditioning of Log Transmissivity by a Concentration Measurement

We wish to illustrate first the general approach for the particular case $B = Y'(\mathbf{x})$, the log transmissivity fluctuation. In applications the calculation of $\langle Y'^c(\mathbf{x}) \rangle$ and $\sigma_Y^{2,c}(\mathbf{x})$ may be of interest in the solution of the inverse problem, i.e., identifica-

tion of the heterogeneous structure with the aid of measurements of concentration.

To simplify the procedure we make the following assumptions:

1. The flow is two-dimensional; i.e., $Y = m_Y + Y'$ is the log transmissivity, and $\mathbf{x}(x_1, x_2)$ are coordinates in the horizontal plane. As already mentioned, Y is normal and stationary, the flow is driven by an averaged constant head gradient $-\mathbf{J}$, and it is uniform in the mean.

2. A first-order approximation in σ_Y^2 is used in order to solve the flow problem. This leads [e.g., Dagan, 1984] to the following relationships:

$$\mathbf{U} = \frac{1}{n} \exp(m_Y) \mathbf{J} \quad \mathbf{u}(\mathbf{x}) = \mathbf{U} Y'(\mathbf{x}) - \frac{\mathbf{U}}{J} \nabla h(\mathbf{x}) \quad (15)$$

where n is the porosity and $h(\mathbf{x})$, the pressure head fluctuation, satisfies the equation resulting from $\nabla \cdot \mathbf{u} = 0$,

$$\nabla^2 h = \mathbf{J} \cdot \nabla Y' \quad (16)$$

These equations permit determining the various covariances $C_{YC}(\mathbf{r}) = \langle Y'(\mathbf{x}) h(\mathbf{y}) \rangle$, $C_H(\mathbf{r})$, $C_{u,Y}(\mathbf{r})$, $u_{ij}(\mathbf{r}) = \langle u_i(\mathbf{x}) u_j(\mathbf{y}) \rangle$, \dots , in a closed form with the aid of the fundamental scalar functions P and Q that satisfy $\nabla^2 P = -C_Y$, $\nabla^2 Q = P$. Examples of such calculations for an exponential $C_Y = \sigma_Y^2 \exp(-r/I_Y)$ can be found in previous studies [Dagan, 1984, 1991; Rubin, 1991].

3. The same first-order approximation is adopted for the kinematic equation (5) leading in $\mathbf{X} = \mathbf{a} + \mathbf{U}t + \mathbf{X}'(t, \mathbf{a})$ to

$$\mathbf{X}'(t, \mathbf{a}) = \int_0^t \mathbf{u}(\mathbf{a} + \mathbf{U}t') dt' \quad (17)$$

That is, the actual trajectory $\mathbf{X}(t)$ is replaced in the argument of \mathbf{u} in (17) by its mean. Assumptions 1 and 2 have led to closed form expression in the past for various moments of X'_i , for example,

$$\begin{aligned} X_{ij}(t) &= \langle X'_i(t, \mathbf{a}) X'_j(t, \mathbf{a}) \rangle = \int_0^t \int_0^t u_{ij}[\mathbf{U}(t' - t'')] dt' dt'' \\ &= 2 \int_0^t (t - t') u_{ij}(\mathbf{U}t') dt' \quad (i, j = 1, 2) \end{aligned} \quad (18)$$

It is emphasized that X_{ij} in (18) is of the order of σ_Y^2 and the neglected terms are of higher order; i.e., X_{ij} in (18) is a first-order term in a consistent expansion in σ_Y^2 .

4. Since \mathbf{u} , h , and \mathbf{X}' result from linear operations on Y' , they are normal under the first-order approximation of assumptions 2 and 3. As a matter of fact, \mathbf{X}' tends to normality for large travel times Ut/I_Y under more general conditions, by virtue of the central limit theorem. Under these conditions the joint pdf of the trajectory components $X_1(t, \mathbf{a})$, $X_2(t, \mathbf{a})$ and of the other variables of interest are multivariate normal and completely characterized by the mean and variance-covariance matrix.

5. Finally, in order to simplify the calculations we select a Gaussian $C_Y(\mathbf{r})$,

$$C_Y(\mathbf{r}) = \sigma_Y^2 \exp(-\pi r^2 / 4 I_Y^2) \quad (19)$$

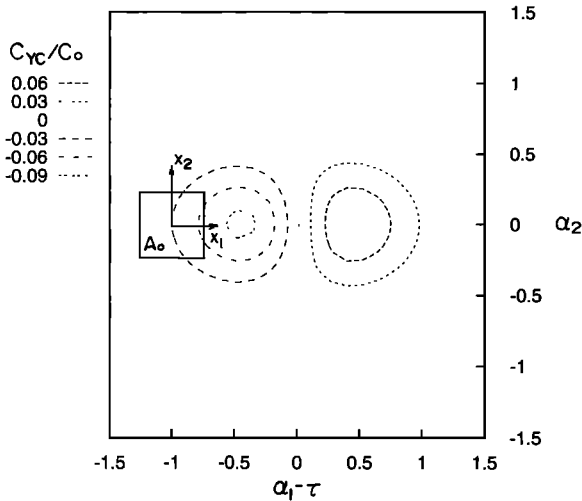


Figure 2. The dependence of the cross covariance C_{YC}/C_0 (equation (20)) between the log transmissivity $Y(x_1, x_2)$ and the concentration $C(\alpha_1, \alpha_2, \tau)$ upon α_1, α_2 . The values of the dimensionless parameters are $l_1 = l_2 = 0.5$, $\sigma_Y^2 = 0.5$, $\tau = 1$, and $x_1 = x_2 = 0$.

and a rectangular input zone A_0 of side l_1, l_2 , $-l_1/2 < a_1 < l_1/2$, $-l_2/2 < a_2 < l_2/2$ (Figure 1).

The first covariance of interest, $C_{YC}(\mathbf{x}, \alpha, \tau) = \langle Y'(\mathbf{x})C(\alpha, \tau) \rangle$, is given by (8) as follows:

$$C_{YC}(x_1, x_2, \alpha_1, \alpha_2, \tau) = C_0$$

$$\cdot \int_{-\infty}^{\infty} \int_{-l_2/2}^{l_2/2} \int_{-l_1/2}^{l_1/2} Y' f(Y', \alpha_1, \alpha_2; x_1, x_2, a_1, a_2, \tau) da_1 da_2 dY' \quad (20)$$

where $f(Y', \alpha_1, \alpha_2; x_1, x_2, a_1, a_2, \tau)$ is the trivariate normal pdf of $Y'(x_1, x_2)$, $X_1(\tau; \mathbf{a}) = \alpha_1$, and $X_2(\tau; \mathbf{a}) = \alpha_2$. The latter and the integration over Y' could be computed analytically, and the derivation is given in Appendix A. C_{YC} was obtained by two numerical quadratures over a_1 and a_2 (see equation (A11)).

To illustrate the results, we depict in Figure 2 lines of constant C_{YC}/C_0 for the following data: $l_1 = l_2 = 0.5$, $x_1 = x_2 = 0$, $\sigma_Y^2 = 0.5$, and $\tau = 1$. Here and in the sequel all variables are made dimensionless with respect to I_Y in (19) and I_Y/U , as scales of length and time, respectively. Besides, the mean flow is in the direction x_1 . In Figure 2 we have depicted C_{YC}/C_0 as a function of the position of the concentration measurement point coordinates α_1 and α_2 .

To grasp the impact of the measurement $C(\alpha_1, \alpha_2, \tau)$ upon $Y'(0, 0)$, we examine first the behavior of C_{YC} for $\alpha_2 = 0$, i.e., along the mean trajectory which passes through the point of reference of Y' . It is seen in Figure 3 that $C_{YC} = 0$ for $\alpha_1 = \tau = 1$, it is negative for $\alpha_1 < 1$, and it is positive for $\alpha_1 > 1$. This is to be expected, since a positive fluctuation Y' causes a positive velocity fluctuation u_1 , which in turn is associated with a solute travel time to the observation point smaller than the mean travel time, i.e., with $\tau < \alpha_1$ or $\alpha_1 - 1 > 0$. On the other hand, C_{YC} tends to zero for a concentration measurement point far from the Y' reference point; i.e., C_{YC} has a maximum for $\alpha_1 > 1$ and a minimum for $\alpha_1 < 1$. The stronger conditioning in the $\alpha_1 < 1$ portion is due to the closeness to the Y'

point in this example. Finally, the decay of C_{YC} with α_2 is due to the drop of correlation between Y' and velocity or trajectory with distance from the origin. The values of C_{YC}/C_0 may be higher than those in Figure 2 for smaller τ and α_1 , i.e., for measurement of concentration closer to the Y' reference point, for smaller l_1 and l_2 , and for larger σ_Y^2 . A detailed analysis of the impact of these parameters, as well as of the coordinates x_1, x_2 of Y' , is beyond the scope of this article.

We switch now to the discussion of the behavior of $\langle Y'^c(x_1, x_2; \alpha_1, \alpha_2, \tau) \rangle = \langle Y^c \rangle - m_Y$, the conditional mean, which is given by equation (10) as follows:

$$\langle Y'^c(x_1, x_2 | \alpha_1, \alpha_2, \tau) \rangle = C_{YC}(x_1, x_2, \alpha_1, \alpha_2, \tau) / \langle C(\alpha_1, \alpha_2, \tau) \rangle \quad (21)$$

The mean concentration $\langle C \rangle$ in (3) could be evaluated in a closed form (equation (A12)). Hence $\langle Y'^c \rangle$ can be readily evaluated with the aid of C_{YC} and $\langle C \rangle$. In Figure 3 we have represented $\langle Y'^c \rangle$ as a function of x_1 and x_2 for $\tau = 1$ and fixed $\alpha_1 = 1.2$ and $\alpha_2 = 0$, other parameters being equal to those of Figure 2. In words, Figure 3 shows the impact of measuring $C = C_0$ at a point on the mean centroid trajectory $\alpha_2 = 0$ and at a time τ that is smaller than the mean travel time, $t = 1.2$, needed to reach α_1 . It is clear that this accelerating effect is achieved by a positive deviation $\langle Y'^c \rangle$, to be added to m_Y . It is also clear from Figure 4 that the impact of $C(\alpha, \tau)$ is larger for log transmissivity at a point \mathbf{x} between the source A_0 and the concentration measurement point than downstream of it. It is also interesting to note that sufficiently far sideways, for $|x_2| > 1$, $\langle Y'^c \rangle$ is negative. Physically, this result can be attributed to the effect of a block of higher conductivity, which slows down particles traveling on streamlines that circumvent the block, in contrast with those that cross it. Finally, it is interesting to note that for this particular configuration, conditioning has a significant impact upon $\langle Y'^c \rangle$, its maximum deviation being of the order of $\sigma_Y/3$.

Finally, we have examined for the same data as in Figure 3, the reduction of the variance of Y owing to conditioning by $C(\alpha, \tau) = C_0$. The computations based on (11) are described in Appendix A. They require two numerical quadratures, leading to the results displayed in Figure 4. The latter presents the

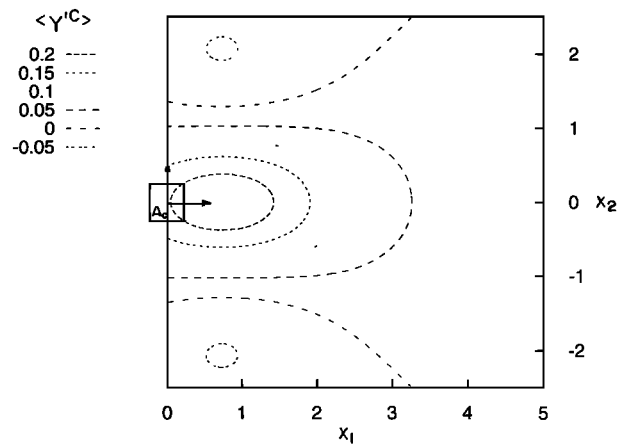


Figure 3. The dependence of the mean conditional log transmissivity fluctuation $\langle Y'^c(x_1, x_2 | \alpha_1, \alpha_2, \tau) \rangle$ (equation (21)) upon x_1, x_2 for $l_1 = l_2 = 0.5$, $\sigma_Y^2 = 0.5$, $\tau = 1$, $\alpha_1 = 1.2$, and $\alpha_2 = 0$.

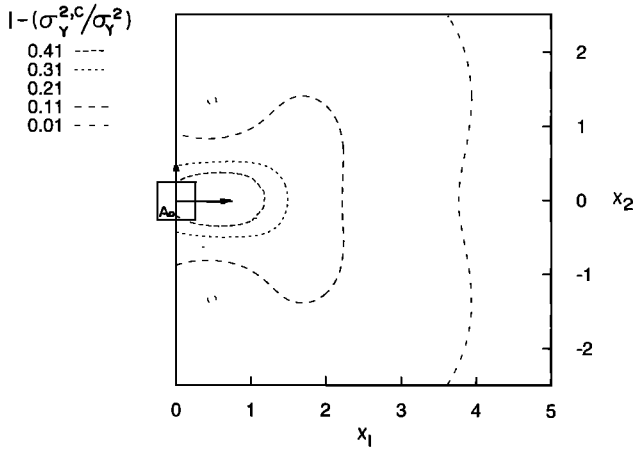


Figure 4. Same data as in Figure 3 for reduction of log transmissivity variance (equation (11)).

coefficient of reduction of the unconditional variance $\sigma_Y^2 = 0.5$ to the conditional one $\sigma_Y^{2,c}$. As in Figure 4, the largest impact of the concentration measurement is achieved in the region $0 < x_1 < \alpha_1$ between the source and the concentration measurement point. Again, for this configuration, the uncertainty reduction is quite large, up to $0.5\sigma_Y^2$.

5. Conditioning of Plume Centroid Trajectory by a Concentration Measurement

To further illustrate our general procedure, we have considered the impact of a measurement $C(\alpha, \tau) = C_0$ upon $B = R_1(t)$ or $B = R_2(t)$, where $\mathbf{x} = \mathbf{R}(t)$ in (4) is the plume centroid trajectory. We have adopted the same simplifying assumptions 1–5 of section 4, and the methodology is similar to that leading to $\langle Y^c \rangle$ and $\sigma_Y^{2,c}$.

The joint pdf $f(R_i, \alpha_1, \alpha_2; t, \tau, a_1, a_2)$, of $R_i(t)$ and

$X_1(\tau, \mathbf{a}) = \alpha_1$, $X_2(\tau, \mathbf{a}) = \alpha_2$ is trivariate normal. For A_0 centered at the origin $\langle R_1 \rangle = t$, $\langle R_2 \rangle = 0$, whereas $\langle X_1(\tau, \mathbf{a}) \rangle = a_1 + \tau$, $\langle X_2(\tau, \mathbf{a}) \rangle = a_2$.

The conditional mean centroid trajectories are given by (10),

$$\langle R_i^c(t|\alpha, \tau) \rangle = \langle R_i(t) \rangle + \frac{C_{R,C}(t, \alpha, \tau)}{\langle C(\alpha, \tau) \rangle} \quad (22)$$

The cross covariance,

$$C_{R,C} = C_0$$

$$\int_{-\infty}^{\infty} \int_{-l_2/2}^{l_2/2} \int_{-l_1/2}^{l_1/2} R_i' f(R_i', \alpha_1, \alpha_2; t, a_1, a_2, \tau) da_1 da_2 dR_i'$$

is evaluated in Appendix B. Ultimately, it requires four quadratures over a_1, a_2 , but for a sufficiently small input zone ($l_1 = l_2 < 0.6$) the integrations can be reduced to two. Similarly, the conditional variance (see equation (11)) requires computing

$$\langle R_i'^2(t) C(\alpha, \tau) \rangle = C_0$$

$$\int_{-\infty}^{\infty} \int_{-l_2/2}^{l_2/2} \int_{-l_1/2}^{l_1/2} R_i'^2 f(R_i', \alpha_1, \alpha_2; t, a_1, a_2, \tau) da_1 da_2 dR_i'$$

which is again accomplished in Appendix B in terms of four quadratures, or two for $l_1 = l_2 < 0.6$.

To illustrate the impact of a concentration measurement, we have chosen to compute $\langle R_2^c(t) \rangle$ and $\sigma_{R_2}^{2,c}(t) = R_{22}^c(t)$ for data similar to those of Figures 3 and 4. Thus we have selected $l_1 = l_2 = 0.5$, $\sigma_Y^2 = 0.5$ and $\tau = 1$. The concentration measurement is supposed to be at $\alpha_1 = \tau = 1$ and $\alpha_2 = 0.5$. It is emphasized that the latter value implies a relatively large sideways deviation of the plume from its main trajectory, and we chose it in order to better illustrate the conditioning effect.

In Figure 5 we have represented both the unconditional

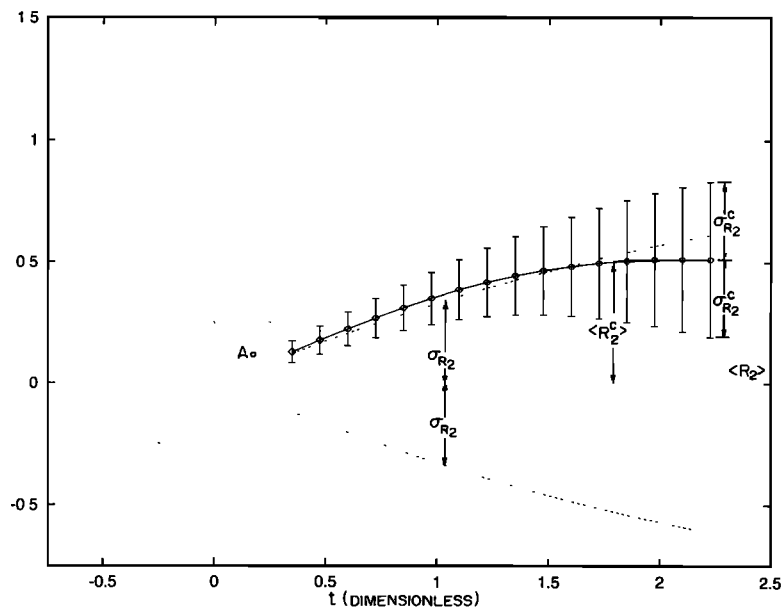


Figure 5. The dependence of the unconditional moments of the plume centroid trajectory $\langle R_2 \rangle$, $\sigma_{R_2}^2(t)$ and the conditional ones, $\langle R_2^c(t|\alpha_1, \alpha_2, \tau) \rangle$ (equation (36)) and $\sigma_{R_2}^{2,c}(t|\alpha_1, \alpha_2, \tau)$ (equation (11)), upon time. Parameter values are $l_1 = l_2 = 0.5$, $\sigma_Y^2 = 0.5$, $\tau = 1$, $\alpha_1 = 1$, and $\alpha_2 = 0.5$.

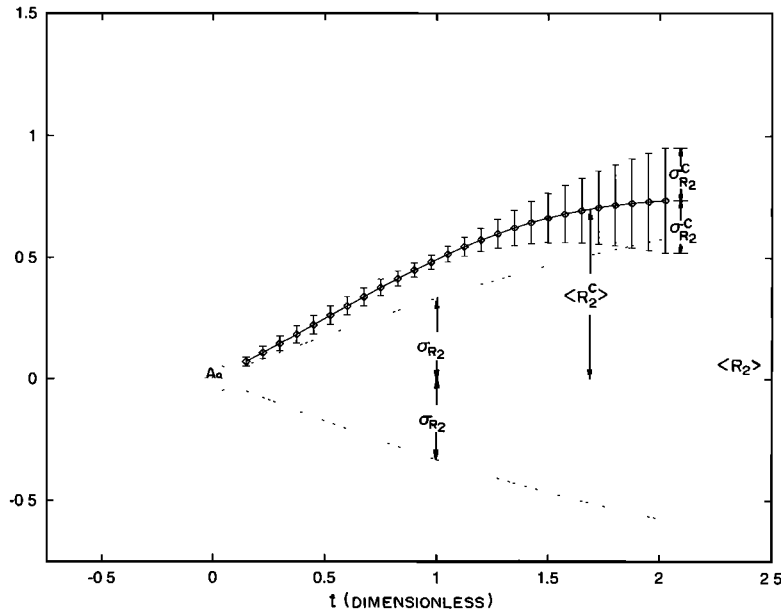


Figure 6. Same as Figure 5 for $l_1 = l_2 = 0.1$.

$\langle R_2 \rangle = 0$, $\sigma_{R_2}^2(t) = R_{22}(t)$ (equation (B2)) and the conditional $\langle R_2^c(t) \rangle$ (22), $\sigma_{R_2^c}^2(t) = R_{22}^c(t)$ as functions of time. First, the relatively large σ_{R_2} implies lack of ergodicity, which is quite expectable for the relatively small plume size [Dagan, 1991]. The most dramatic effect of conditioning is indeed the sidewise deviation of the mean centroid trajectory. This is to be expected, since $C(\alpha, \tau) = C_0$ reduces the subensemble of realizations to those for which at least one trajectory emanating from A_0 passes through the conditioning point at $t = \tau$. The same constraint causes a significant reduction of the variance from its unconditional $\sigma_{R_2}^2$ to the conditional $\sigma_{R_2^c}^2$. The impact is larger upstream of the measurement point and dissipates as the solute body moves past the conditioning point.

To further illustrate the impact of the solute body size, we have computed σ_{R_2} , $\langle R_2^c \rangle$, $\sigma_{R_2^c}^2$ for same parameter values, except that $l_1 = l_2 = 0.1$, and have represented them in Figure 6. Such a small solute body is convected but does not disperse [Dagan, 1991]. Since conditioning by $C(1, 1, 1) = C_0$ forces the solute body to pass through $\alpha_1 = 1$, $\alpha_2 = 1$ at $t = \tau = 1$, the trajectory $\langle R_2^c \rangle$ is strongly conditioned by this constraint, and the same is true for the variance $\sigma_{R_2^c}^2$, which is reduced practically to $l_2/2$ or less, upstream of the concentration measurement point, and starts to increase quickly for $t > 1$.

6. Summary and Conclusions

The present study is concerned with the effect of concentration measurements upon identification of aquifer properties and upon predicting the further evolution of the plume. By adopting a Lagrangian approach, concentration is related to particle trajectories, and conditioning by a measurement is converted into limiting the realizations of the trajectory fields to those for which at least one trajectory passes through the measurement point $\mathbf{x} = \alpha$ at the given time $t = \tau$. This statement is cast in a mathematical form by defining first the pdf of the initial coordinates \mathbf{a} of all trajectories that pass through $\mathbf{x} = \alpha$ at $t = \tau$ (the so-called backward probability). Thus, conditioning by a concentration measurement is equivalent to limiting the random variable \mathbf{a} to be confined in the initial solute body A_0 . Along this line, any random variable

$B(\mathbf{x}, t)$ (e.g., log conductivity, head, velocity, and plume centroid) that is correlated to trajectories can be conditioned by a concentration measurement. It is shown that this approach leads to the same conditional mean as the one obtained by cokriging B with concentration, whereas the conditional variance of B derived by cokriging is not correct. For instance, the conditional variances derived here differ depending on whether the measured concentration is equal to that of the plume or is zero, whereas cokriging does not discriminate between the two. This discrepancy is attributed to C having a binomial pdf for fixed \mathbf{x} , t or to C being an indicator function of \mathbf{x} for a fixed t . By adopting a few simplifying assumptions we were able to illustrate the procedure by deriving the expressions of the conditional mean and variances of the log transmissivity and of the plume centroid trajectories and to grasp a few of their proprieties.

The present study is only a first step toward a more comprehensive assessment of the impact of concentration measurements. Future theoretical developments have to address a few issues such as the presence of a few measurement points, continuous time monitoring, the influence of pore-scale dispersion, three-dimensional flow and transport, and effect of space averaging of concentration.

It is emphasized that conditioning has a significant impact for large heterogeneity scales compared to the plume scale and for scarce measurements. In contrast, for the field experiments carried out in the past, in which plumes were monitored extensively in space and time, the identification of the formation structure and of plume spatial moments achieved by a best fit with unconditional transport solutions was simple and quite accurate.

Appendix A: Derivation of the Log Transmissivity Conditional Moments

With x_1 the direction parallel to the mean flow, we have

$$X_1(t, \mathbf{a}) = a_1 + Ut + X'_1(t, \mathbf{a}) \quad X_2(t, \mathbf{a}) = a_2 + X'_2(t, \mathbf{a})$$

The conditional joint pdf of $Y'(\mathbf{x}) = Y(\mathbf{x}) - m_Y$, $X_1(\tau, \mathbf{a})$ and $X_2(\tau, \mathbf{a})$ was assumed to be trivariate normal. It is com-

pletely defined by the mean $\langle Y' \rangle = 0$, $\langle X_1 \rangle = a_1 + U\tau$, $\langle X_2 \rangle = a_2$ and the variance-covariance matrix

$$\begin{bmatrix} \sigma_Y^2 & C_{X_1Y} & C_{X_2Y} \\ C_{X_1Y} & X_{11} & 0 \\ C_{X_2Y} & 0 & X_{22} \end{bmatrix}$$

where

$$X_{11}(\tau) = \langle X_1'^2(\tau, \mathbf{a}) \rangle = \int_0^\tau \int_0^\tau u_{11}[U(t' - t''), 0] dt' dt'' \quad (\text{A1})$$

$$X_{22}(\tau) = \int_0^\tau \int_0^\tau u_{22}[U(t' - t''), 0] dt' dt'' \quad X_{12}(\tau) = 0$$

are the trajectory variances and u_{ij} are the velocity covariances. X_{11} and X_{22} were computed analytically for a Gaussian log conductivity covariance $C_Y = \sigma_Y^2 \exp(-\pi r^2/4I_Y^2)$ by the procedure outlined in previous studies for an exponential covariance [Dagan, 1982]. The final result is written with the aid of dimensionless variables Ut/I_Y , \mathbf{x}/I_Y , \dots as follows:

$$X_{11}(\tau) = 2\sigma_Y^2 \left[\tau \operatorname{erf} \left(\tau \frac{\pi^{1/2}}{2} \right) + \frac{2}{\pi} \exp \left(-\frac{\pi \tau^2}{4} \right) - \frac{2}{\pi} + p(\tau, 0) + \frac{1}{\tau} \frac{dq(\tau, 0)}{d\tau} \right] \quad (\text{A2})$$

$$X_{22}(\tau) = -\sigma_Y^2 \frac{2}{\tau} \frac{dq(\tau, 0)}{d\tau} \quad (\text{A3})$$

where

$$p(r_1, r_2) = \frac{1}{\pi} \left[E_i \left(-\frac{\pi}{4} r^2 \right) - \ln \left(\frac{\pi}{4} r^2 \right) - E \right] \quad (\text{A4})$$

$$\frac{d}{dr} q(r_1, r_2) = \frac{1}{\pi} \left\{ \frac{r}{2} \left[E_i \left(-\frac{\pi}{4} r^2 \right) - \ln \left(\frac{\pi}{4} r^2 \right) - E \right] + \frac{r}{2} - \frac{2}{r\pi} \left[1 - \exp \left(-\frac{\pi r^2}{4} \right) \right] \right\} \quad (\text{A5})$$

with

$$E_i(-z) = -\int_z^{+\infty} \frac{e^{-t}}{t} dt \quad E = 0.577216 \quad r = (r_1^2 + r_2^2)^{1/2}$$

The cross covariance $C_{YX_1} = \langle X_1'(\tau, \alpha) Y'(\mathbf{x}) \rangle$ is expressed in terms of the velocity-log conductivity cross covariance $C_{u_1Y}(\alpha_1 + \tau - x_1, \alpha_2 - x_2) = \langle u_1(\alpha_1 + \tau, \alpha_2) Y'(x_1, x_2) \rangle$ as follows:

$$C_{X_1Y}(\mathbf{x}, \alpha, \tau) = \int_0^\tau C_{u_1Y}(\alpha_1 + t - x_1, \alpha_2 - x_2) dt \quad (\text{A6})$$

The velocity-log conductivity covariance can be computed with the aid of the Y and H (the head) covariance by the procedure outlined previously [Dagan, 1984; Rubin, 1991]. For a Gaussian C_Y the final result is

$$C_{u_1Y}(\mathbf{x}, \alpha, \tau) = \sigma_Y^2 \left\{ \exp \left(-\frac{\pi r^2}{4} \right) \left[1 - \frac{r_1^2}{r^2} - \frac{2r_1^2}{\pi r^4} \right] \right.$$

$$\left. + \frac{2r_1^2}{\pi r^4} + \frac{r^2 - 2r_1^2}{r^3} \frac{dp(r_1, r_2)}{dr} \right\} \quad (\text{A7})$$

$$C_{X_1Y}(\mathbf{x}, \alpha, \tau) = \sigma_Y^2 \left\{ e^{-\pi^2/4} \left[\operatorname{erf} \left(\frac{\pi^{1/2} r_1}{2} \right) - \operatorname{erf} \left(\frac{\pi^{1/2}}{2} (\alpha_1 - x_1) \right) \right] \right.$$

$$\left. + \frac{r_1}{(r_1^2 + r_2^2)^{1/2}} \frac{dp(r_1, r_2)}{dr} - \frac{(\alpha_1 - x_1)}{[(\alpha_1 - x_1)^2 + r_2^2]^{1/2}} \frac{dp(\alpha_1 - x_1, r_2)}{dr} \right\} \quad (\text{A8})$$

with

$$r_1 = \alpha_1 + \tau - x_1 \quad r_2 = \alpha_2 - x_2$$

By a similar procedure,

$$C_{u_2Y}(\mathbf{x}, \alpha, \tau) = \sigma_Y^2 \left\{ \frac{2r_1 r_2}{\pi r^4} - \frac{r_1 r_2}{r^2} \exp \left(-\frac{\pi r^2}{4} \right) \left[1 + \frac{2}{\pi r^2} \right] \right.$$

$$\left. - \frac{r_1 r_2}{r^3} \frac{dp(r_1, r_2)}{dr} \right\} \quad (\text{A9})$$

$$C_{X_2Y}(\mathbf{x}, \alpha, \tau) = \sigma_Y^2 \left\{ \frac{\partial p(\alpha_1 + \tau - x_1, r_2)}{\partial r_2} - \frac{\partial p(\alpha_1 - x_1, r_2)}{\partial r_2} \right\} \quad (\text{A10})$$

After these preparatory steps, to obtain $C_{YC}(\mathbf{x}, \alpha, \tau) = \langle Y'(\mathbf{x}) C(\alpha, \tau) \rangle$ in (20), we have to integrate the trivariate normal $f(Y', \alpha_1, \alpha_2; \mathbf{x}, \alpha, \tau)$ over Y' and \mathbf{a} . The first integration could be done analytically, yielding the final result

$$C_{YC}(\mathbf{x}, \alpha, \tau) = \frac{C_0}{2\pi(X_{11}X_{22})^{1/2}} \int_{-l_1/2}^{l_1/2} \int_{-l_2/2}^{l_2/2} \exp \left\{ -\frac{1}{2} \left[\frac{\alpha_1'^2}{X_{11}} + \frac{\alpha_2'^2}{X_{22}} \right] \right\}$$

$$\cdot \left[\frac{C_{X_1Y}}{X_{11}} \alpha_1' + \frac{C_{X_2Y}}{X_{22}} \alpha_2' \right] da_1 da_2 \quad (\text{A11})$$

where $\alpha_1' = \alpha_1 - \tau - a_1$ and $\alpha_2' = \alpha_2 - a_2$. Two numerical quadratures in (A11) led to the results displayed in Figure 2.

To obtain the conditional mean $\langle Y'^c(\mathbf{x}|\alpha, \tau) \rangle$ in (21), we need to divide C_{YC} in (A11) by $\langle C(\alpha, \tau) \rangle$. This is given by (3) and has the simple expression

$$\langle C(\alpha, \tau) \rangle = C_0 \int_{-l_1/2}^{l_1/2} \int_{-l_2/2}^{l_2/2} f(\alpha_1, \alpha_2; \tau, a_1, a_2) da_1 da_2$$

$$= \frac{1}{4} \left[\operatorname{erf} \left(\frac{\alpha_1 + \frac{l_1}{2} - \tau}{(2X_{11})^{1/2}} \right) - \operatorname{erf} \left(\frac{\alpha_1 - \frac{l_1}{2} - \tau}{(2X_{11})^{1/2}} \right) \right]$$

$$\cdot \left[\operatorname{erf} \left(\frac{\alpha_2 + \frac{l_2}{2}}{(2X_{22})^{1/2}} \right) - \operatorname{erf} \left(\frac{\alpha_2 - \frac{l_2}{2}}{(2X_{22})^{1/2}} \right) \right] \quad (\text{A12})$$

where $f(\alpha_1, \alpha_2; \tau, a_1, a_2)$ is the joint pdf of $X_1(\tau, \mathbf{a})$, $X_2(\tau, \mathbf{a})$ for $X_1 = \alpha_1$, $X_2 = \alpha_2$. Equations (21), (3), (A11), and (A12) were used for plotting $\langle Y'^c(\mathbf{x}|\alpha, t) \rangle$ in Figure 3.

Finally, to derive the conditional variance $\sigma_Y^{2,c}(\mathbf{x}|\alpha, t)$ in (11), we need to integrate the trivariate $f(Y', \alpha_1, \alpha_2; \tau, a_1, a_2)$ over Y'^2 , the result being now

$$\begin{aligned}
& \langle Y'^2(\mathbf{x})C(\alpha, \tau) \rangle \\
&= \frac{C_0}{2\pi(X_{11}X_{22})^{1/2}} \int_{-l_1/2}^{l_1/2} \int_{-l_2/2}^{l_2/2} \exp \left\{ -\frac{1}{2} \left[\frac{\alpha_1'^2}{X_{11}} - \frac{\alpha_2'^2}{X_{22}} \right] \right\} \\
&\cdot \left[\sigma_Y^2 - \frac{C_{X_1Y}^2}{X_{11}} - \frac{C_{X_2Y}^2}{X_{22}} + \left(\frac{C_{X_1Y}}{X_{11}} \alpha_1' + \frac{C_{X_2Y}}{X_{22}} \alpha_2' \right)^2 \right] da_1 da_2 \quad (A13)
\end{aligned}$$

After numerical quadratures, (A10), (A11), and (A13) were used to calculate the values of σ_Y^2 displayed in Figure 5.

Appendix B: Derivation of the Plume Centroid Trajectory Conditional Moments

With the centroid coordinates defined by (4), i.e., $\langle R_1 \rangle = t$, $\langle R_2 \rangle = 0$,

$$R'_i(t) = \frac{1}{l_1 l_2} \int_{-l_1/2}^{l_1/2} \int_{-l_2/2}^{l_2/2} X'_i(t, \mathbf{b}) db_1 db_2 \quad (B1)$$

we must first evaluate the trivariate normal pdf of $R'_i(t)$, $X_1(\tau, \mathbf{a})$, $X_2(\tau, \mathbf{a})$. The pdf is defined by the mean $\langle R'_i \rangle = 0$, $\langle X_1 \rangle = a_1 + U\tau$, $\langle X_2 \rangle = a_2$ and the variance-covariance matrix

$$\begin{bmatrix} R_u & C_{R,X_1} & C_{R,X_2} \\ C_{R,X_1} & X_{11} & 0 \\ C_{R,X_2} & 0 & X_{22} \end{bmatrix}$$

Again, adopting the Gaussian C_Y leads to X_{11} and X_{22} in (A1) and (A2). The centroid covariance is given by

$$\begin{aligned}
R_y(t) &= \frac{1}{l_1^2 l_2^2} \\
&\cdot \int_{-l_1/2}^{l_1/2} \int_{-l_1/2}^{l_1/2} \int_{-l_2/2}^{l_2/2} \int_{-l_2/2}^{l_2/2} X_y(t, t, \mathbf{a}, \mathbf{b}) da_1 da_2 db_1 db_2 \quad (B2)
\end{aligned}$$

where

$$\begin{aligned}
X_y(t, \tau, \mathbf{a}, \mathbf{b}) &= \langle X'_i(t, \mathbf{a}) X'_i(\tau, \mathbf{b}) \rangle = \int_0^t \int_0^\tau u_y [U(t' - t'') \\
&\quad + a_1 - b_1, a_2 - b_2] dt' dt'' \quad (B3)
\end{aligned}$$

The two-point covariance X_{11} and X_{22} in (A3) could be derived in a closed form as follows:

$$\begin{aligned}
X_{11}(t, \tau, \mathbf{a}, \mathbf{b}) &= \exp \left(-\frac{\pi}{4} (b_2 - a_2)^2 \right) \\
&\cdot \left\{ \frac{2}{\pi} \left[\exp \left(-\frac{\pi}{4} (a_1 - b_1 - \tau)^2 \right) \right. \right. \\
&\quad + \exp \left(-\frac{\pi}{4} (a_1 - b_1 + t)^2 \right) - \exp \left(-\frac{\pi}{4} (a_1 - b_1)^2 \right) \\
&\quad \left. \left. - \exp \left(-\frac{\pi}{4} (a_1 - b_1 + t - \tau)^2 \right) \right] \right. \\
&\quad \left. + (a_1 - b_1 - \tau) \operatorname{erf} \left[\frac{\pi^{1/2}}{2} (a_1 - b_1 - \tau) \right] \right.
\end{aligned}$$

$$\begin{aligned}
&- (a_1 - b_1 + t - \tau) \operatorname{erf} \left[\frac{\pi^{1/2}}{2} (a_1 - b_1 + t - \tau) \right] \\
&+ (a_1 - b_1 + t) \operatorname{erf} \left[\frac{\pi^{1/2}}{2} (a_1 - b_1 + t) \right] \\
&- (a_1 - b_1) \operatorname{erf} \left[\frac{\pi^{1/2}}{2} (a_1 - b_1) \right] \Big\} \\
&+ \left[2 - \frac{(a_1 - b_1 - \tau)^2}{(a_1 - b_1 - \tau)^2 + (a_1 - b_1)^2} \right] \\
&\cdot p(a_1 - b_1 - \tau, a_2 - b_2) \\
&+ \left[2 - \frac{(a_1 - b_1 + t)^2}{(a_1 - b_1 + t)^2 + (a_1 - b_1)^2} \right] \\
&\cdot p(a_1 - b_1 + t, a_2 - b_2) \\
&- \left[2 - \frac{(a_1 - b_1 + t - \tau)^2}{(a_1 - b_1 + t - \tau)^2 + (a_1 - b_1)^2} \right] \\
&\cdot p(a_1 - b_1 + t - \tau, a_2 - b_2) - 2p(a_1 - b_1, a_2 - b_2) \\
&- \frac{(a_2 - b_2)^2 - (a_1 - b_1 - \tau)^2}{\{[(a_1 - b_1 - \tau)^2 + (a_2 - b_2)^2]^{1/2}\}^3} \\
&\cdot \frac{d}{dr} q(a_1 - b_1 - \tau, a_2 - b_2) \\
&- \frac{(a_2 - b_2)^2 - (a_1 - b_1 + t)^2}{\{[(a_1 - b_1 + t)^2 + (a_2 - b_2)^2]^{1/2}\}^3} \\
&\cdot \frac{d}{dr} q(a_1 - b_1 + t, a_2 - b_2) \\
&+ \frac{(a_2 - b_2)^2 - (a_1 - b_1 + t - \tau)^2}{\{[(a_1 - b_1 + t - \tau)^2 + (a_2 - b_2)^2]^{1/2}\}^3} \\
&\cdot \frac{d}{dr} q(a_1 - b_1 + t - \tau, a_2 - b_2) \\
&+ \frac{(a_2 - b_2)^2 - (a_1 - b_1)^2}{\{[(a_1 - b_1)^2 + (a_2 - b_2)^2]^{1/2}\}^3} \\
&\cdot \frac{d}{dr} q(a_1 - b_1, a_2 - b_2) \quad (B4)
\end{aligned}$$

$$\begin{aligned}
X_{22}(t, \tau, \mathbf{a}, \mathbf{b}) &= -\frac{(a_2 - b_2)^2}{(a_1 - b_1 - \tau)^2 + (a_1 - b_1)^2} \\
&\cdot p(a_1 - b_1 - \tau, a_2 - b_2) \\
&- \frac{(a_2 - b_2)^2}{(a_1 - b_1 + t)^2 + (a_1 - b_1)^2} p(a_1 - b_1 + t, a_2 - b_2) \\
&+ \frac{(a_2 - b_2)^2}{(a_1 - b_1 + t - \tau)^2 + (a_1 - b_1)^2} \\
&\cdot p(a_1 - b_1 + t - \tau, a_2 - b_2) \\
&+ \frac{(a_2 - b_2)^2}{(a_1 - b_1)^2 + (a_1 - b_1)^2} p(a_1 - b_1, a_2 - b_2) \\
&- \frac{(a_1 - b_1 - \tau)^2 - (a_2 - b_2)^2}{\{[(a_1 - b_1 - \tau)^2 + (a_2 - b_2)^2]^{1/2}\}^3}
\end{aligned}$$

$$\begin{aligned}
& \cdot \frac{d}{dr} q(a_1 - b_1 - \tau, a_2 - b_2) \\
& - \frac{(a_1 - b_1 + t)^2 - (a_2 - b_2)^2}{\{[(a_1 - b_1 + t)^2 + (a_2 - b_2)^2]^{1/2}\}^3} \\
& \cdot \frac{d}{dr} q(a_1 - b_1 + t, a_2 - b_2) \\
& + \frac{(a_1 - b_1 + t - \tau)^2 - (a_2 - b_2)^2}{\{[(a_1 - b_1 + t - \tau)^2 + (a_2 - b_2)^2]^{1/2}\}^3} \\
& \cdot \frac{d}{dr} q(a_1 - b_1 + t - \tau, a_2 - b_2) \\
& + \frac{(a_1 - b_1)^2 - (a_2 - b_2)^2}{\{[(a_1 - b_1)^2 + (a_2 - b_2)^2]^{1/2}\}^3} \\
& \cdot \frac{d}{dr} q(a_1 - b_1, a_2 - b_2) \quad X_{12} = 0 \quad (B5)
\end{aligned}$$

whereas R_{ij} in (B2) requires numerical quadratures. However, for $l_1 = l_2 < 0.6$ it was found that R_{ij} is given accurately by

$$R_{ij}(t) = \frac{1}{l_1 l_2} \int_{-l_1/2}^{l_1/2} \int_{-l_2/2}^{l_2/2} X_{ij}(t, \mathbf{a}, 0) da_1 da_2$$

The centroid-trajectory covariance, $C_{R_i X_j}(t, \alpha, \tau) = \langle R'_i(t) X'_j(\tau, \alpha) \rangle$, is given by

$$C_{R_i X_j}(t, \alpha, \tau) = \frac{1}{l_1 l_2} \int_{-l_1/2}^{l_1/2} \int_{-l_2/2}^{l_2/2} X_{ij}(t, \tau, \alpha, \mathbf{b}) db_1 db_2 \quad (B6)$$

and $C_{R_i X_j}$ could be determined only numerically, except for $l_1 = l_2 < 0.6$, for which the above approximation applies.

The covariance $C_{R_i C}(t, \alpha, \tau) = \langle R'_i(t) C(\tau, \alpha) \rangle$ needed for determining the conditional mean (22) is formed from the trivariate $f(R'_i, \alpha_1, \alpha_2; t, \tau, \mathbf{a})$. Thus, by using the above results and after integrations over R'_i we get

$$\begin{aligned}
C_{R_1 C}(t, \alpha, \tau) &= \int_{-\infty}^{\infty} \int_{-l_1/2}^{l_1/2} \int_{-l_2/2}^{l_2/2} R'_1 f(R'_1, \alpha_1, \alpha_2; t, \tau, a_1, a_2) da_1 da_2 dR'_1 \\
&= \frac{1}{2\pi(X_{11}X_{22})^{1/2}} \int_{-l_1/2}^{l_1/2} \int_{-l_2/2}^{l_2/2} \exp \left\{ -\frac{1}{2} \left[\frac{\alpha_1'^2}{X_{11}} + \frac{\alpha_2'^2}{X_{22}} \right] \right\} \\
&\quad \cdot \frac{C_{R_1 X_1}}{X_{11}} \alpha_1' da_1 da_2 \quad (B7)
\end{aligned}$$

$$\begin{aligned}
C_{R_2 C}(t, \alpha, \tau) &= \frac{1}{2\pi(X_{11}X_{22})^{1/2}} \\
&\quad \cdot \int_{-l_1/2}^{l_1/2} \int_{-l_2/2}^{l_2/2} \exp \left\{ -\frac{1}{2} \left[\frac{\alpha_1'^2}{X_{11}} + \frac{\alpha_2'^2}{X_{22}} \right] \right\} \frac{C_{R_2 X_2}}{X_{22}} \alpha_2' da_1 da_2 \\
&\quad (B8)
\end{aligned}$$

These two covariances had to be determined by numerical quadratures in order to compute $\langle R_2^c \rangle$ (Figures 5 and 6). In a similar manner the moments for evaluating $\sigma_{R_i}^2(t|\alpha, \tau) = R_{ii}^c(t|\alpha, \tau)$ in (11) are related to

$$\begin{aligned}
& \langle R_i^c(t) C(\alpha, \tau) \rangle \\
&= \int_{-\infty}^{\infty} \int_{-l_1/2}^{l_1/2} \int_{-l_2/2}^{l_2/2} R'_i f(R'_i, \alpha_1, \alpha_2; t, \tau, \mathbf{a}) da_1 da_2 dR'_i \\
&= \frac{1}{2\pi(X_{11}X_{22})^{1/2}} \int_{-l_1/2}^{l_1/2} \int_{-l_2/2}^{l_2/2} \exp \left\{ -\frac{1}{2} \left[\frac{\alpha_1'^2}{X_{11}} + \frac{\alpha_2'^2}{X_{22}} \right] \right\} \\
&\quad \cdot \left[R_{ii} - \frac{C_{R_i X_i}^2}{X_{ii}} \left(1 - \frac{\alpha_i'^2}{X_{ii}} \right) \right] da_1 da_2 \quad (B9)
\end{aligned}$$

The numerical quadrature in (B9) led to the conditional variances illustrated for $R_{22}^c(t, \alpha, \tau)$ in Figures 5 and 6.

Acknowledgments. The work was conducted during the visit of I. Butera and E. Grella at the Tel Aviv University. Thanks are extended to U. Maione and M. G. Tanda of Milan Polytechnic for initiating the visit and to the host institution.

References

- Dagan, G., Stochastic modeling of groundwater flow by unconditional and conditional probabilities, 2, The solute transport, *Water Resour. Res.*, 18, 835–848, 1982.
- Dagan, G., Solute transport in heterogeneous porous formations, *J. Fluid Mech.*, 145, 151–177, 1984.
- Dagan, G., *Flow and Transport in Porous Formations*, 465 pp., Springer-Verlag, New York, 1989.
- Dagan, G., Dispersion of a passive solute in non-ergodic transport by steady velocity fields in heterogeneous formations, *J. Fluid Mech.*, 233, 197–210, 1991.
- Dagan, G., and S. P. Neuman, Nonasymptotic behavior of a common Eulerian approximation for transport in random velocity fields, *Water Resour. Res.*, 27, 3249–3257, 1991.
- Deng, F. W., J. H. Cushman, and J. W. Delleur, Adaptive estimation of the log fluctuating conductivity from tracer data at the Cape Cod site, *Water Resour. Res.*, 29, 4011–4018, 1993a.
- Deng, F. W., J. H. Cushman, and J. W. Delleur, A fast Fourier transform analysis of the contaminant transport problem, *Water Resour. Res.*, 29, 3241–3248, 1993b.
- Graham, W., and D. McLaughlin, Stochastic analysis of nonstationary subsurface solute transport, 1, Unconditional moments, *Water Resour. Res.*, 25, 215–232, 1989a.
- Graham, W., and D. McLaughlin, Stochastic analysis of nonstationary subsurface solute transport, 2, Conditional moments, *Water Resour. Res.*, 25, 2331–2356, 1989b.
- Lee, K. K., F. W. Deng, and J. H. Cushman, Multiscale adaptive estimation of the conductivity field from head and tracer data, *Stochastic Hydraul. Hydrol.*, 7, 66–82, 1993.
- Neuman, S. P., C. L. Winter, and C. M. Newman, Stochastic theory of field-scale Fickian dispersion in anisotropic porous media, *Water Resour. Res.*, 23, 453–466, 1987.
- Rubin, Y., Prediction of tracer plume migration in disordered porous media by the method of conditional probabilities, *Water Resour. Res.*, 27, 1291–1308, 1991.
- Rubin, Y., and G. Dagan, Conditional estimation of solute travel time in heterogeneous formations, 1, Impact of transmissivity measurements, *Water Resour. Res.*, 28, 1033–1044, 1992.
- Thierrin, J., and P. K. Kitanidis, Solute dilution at the Borden and Cape Cod groundwater tracer tests, *Water Resour. Res.*, 30, 2883–2890, 1994.

I. Butera and E. Grella, Department of Hydraulic Engineering, Milan Polytechnic, Milan 20133, Italy. (e-mail: ibara@idra2.iaa.polimi.it)

G. Dagan, Faculty of Engineering, Tel Aviv University, P.O. Box 39040, Ramat-Aviv 69978, Israel. (e-mail: dagan@eng.tau.ac.il)

(Received November 21, 1994; revised August 29, 1995; accepted August 31, 1995.)